Recursive Terrain Navigation with the Correlation Method for High Position Accuracy

Ingemar Nygren, Magnus Jansson
inygren@s3.kth.se, magnus.jansson@s3.kth.se
Department of Signals, Sensors and Systems
Royal Institute of Technology (KTH), Stockholm, Sweden

***Abstract*—In many autonomous underwater vehicle (AUV) applications, there is a need to accurately determine the AUV's position in an effective way in terms of both cost and energy consumption. Since underwater maps are rare there is also a need for navigational methods that can accommodate very infrequent sampling in time and space.**

This paper describes an efficient method to solve above problem by using a multibeam sonar and a linear Kalman filter. The proposed method uses a minimum of underwater maps and is very accurate and robust compared to other methods used for terrain navigation. The achieved 1 σ - circular accuracy (correlation only) is 0.3 - 0.4 meter in the north of the Baltic Sea.

I. INTRODUCTION

In many autonomous underwater vehicle (AUV) applications, there is a need to accurately determine the AUV's position in relation to the underlying bottom structures or in relation to the coordinates on a map in an effective way.

An example of such a civilian application is an AUV approaching an environmental sampling station and an example of a military application is a mine counter measure operation (MCM) where it is vital that the exact position of the mine-like object can be determined.

Some important general issues pertaining to terrain navigation systems for an AUV's are the following:

- Robustness with respect to filter divergence
- Requirements for underwater maps
- Risk of revealing (military applications)
- Accuracy of positioning
- Ability to determine position in flat bottomed areas
- Ability to do own mapping of the bottom topography

Other important questions are:

- Does the system require accurate initialization ?
- Can the system be used by a stationary vehicle ?
- Time for having a position fix from a non-initiated system

An often proposed solution to the positioning problem is to use a method similar to the terrain navigation method used to guide cruise missiles [1]-[4] (see Figure 1).

In the AUV case, an echo-sounder will be used for measuring the depth every, say, 10 meters. The measurements are integrated with an inertial navigation system (INS) by a extended Kalman filter (EKF) or by a Bayesian recursive filter implemented as a mass-point filter or a particle filter [4]. However, these methods are not particularly accurate or

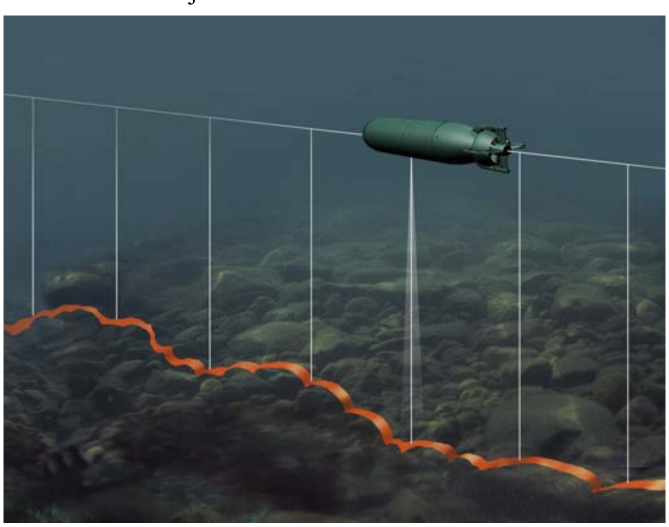

Fig.1. Terrain navigation according to the cruise missile principle. The vehicle is measuring the depth by one sonar beam at each sampling event. Likely positions are positions in the map with the same depth.

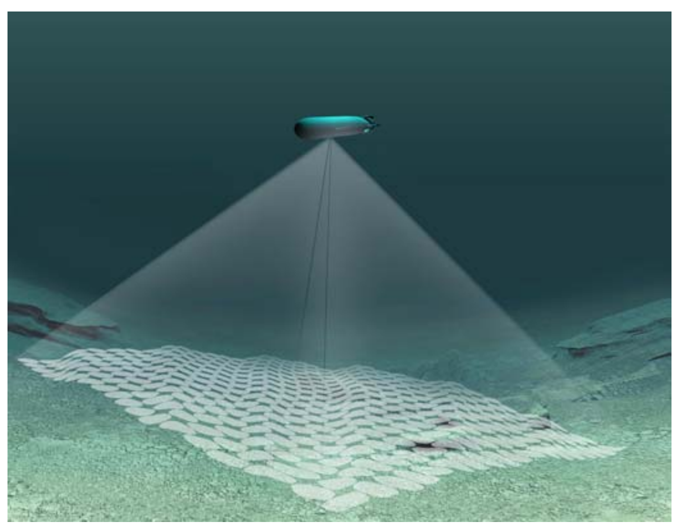

Fig.2. The bottom topography measurement with the correlation method. The vehicle is measuring the bottom topography by several sonar beams. Likely positions are positions with the same bottom topography.

energy-effective since the sonar has to work continuously with a power drain almost as high as for propulsion. This is an important point for battery operated vehicles.

The computational requirements for mass-point and particle filters are also quite high. Furthermore, underwater maps have to be available of the whole area over which the AUV operates.

This paper describes a different method [5], called the correlation method, with high accuracy and a filter with almost optimal performance. The proposed method fulfills the requirements in the point list in previous page. Figure 2 illustrates the method. The measurement is fused with the INS-position with a linear Kalman filter with almost optimal performance.

The sampling frequency of the bottom topography can be very infrequent and the position can often be determined by a single 3D sonar ping. The method is more robust than the conventional terrain navigation with either an extended Kalman filter or a Bayesian recursive filter. The method does not need maps over the whole area of operation area which is a great advantage since high quality underwater maps are rare.

The correlation method has successfully been tested in a non-recursive mode but can of course also be used in a recursive mode. This will greatly improve the performance in very flat areas.

The aim with the paper is to formulate a linear Kalman filter, for non-frequent sampling, for terrain navigation instead of the usual extended Kalman filter.

The paper starts in Section II with comparing recursive Bayesian terrain navigation in two cases. The first case is terrain navigation with only one measuring beam corresponding to using an echo-sounder (cf. Figure 1). The second case corresponds to using a multibeam sonar with several measuring beams (cf. Figure 2). This comparison will give an insight into the great difference between measuring with one beam and measuring with several beams.

Section III discusses the probability of having false likelihood positions because of terrain repeatability. This is an important property since long time between sampling of the bottom topography means that the INS-system no longer can assist in choosing the correct likelihood peak due to the INS-drift.

In order to formulate a near optimal linear Kalman filter we must know if the normalized measurement likelihood function can be approximated by a Gaussian PDF without greater error. The asymptotic properties of the maximum likelihood estimator will provide this information. Section IV discusses therefore the maximum likelihood estimation in this respect.

Section V discusses the formulation of the linear Kalman filter. Section VI gives result from sea-trials and Section VII concludes the article.

II. BAYESIAN RECURSIVE ESTIMATION

Figure 2 shows an underwater vehicle that measures the bottom topography over a large bottom area with a large number of sonar beams at each sampling event. The assumption for the evolution of the state space is

$$\mathbf{x}_{t+1} = \mathbf{x}_t + \mathbf{u}_t + \mathbf{v}_t \qquad t = 1, 2, 3 \dots \tag{1}$$

$$\mathbb{Y}_t = \mathbb{H}(\mathbf{x}_t) + \mathbb{E}_t \tag{2}$$

where $\mathbf{x}_t$ is the position in the horizontal plane at time t and $\mathbf{u}_t$ - the distance between the positions - is provided by the INS system. The measured depths to the bottom are collected in the matrix $\mathbb{Y}_t$ and the matrix $\mathbb{H}(\mathbf{x}_t)$ collects the depths according to the map if we are in position $\mathbf{x}_t$. The error in the INS system is $\mathbf{v}_t$ and $\mathbb{E}_t$ is the error in the depth measurement. The number of measurement points (sonar beams) is N. In order to simplify the discussion we vectorize (2)

$$\mathbf{y}_t = \mathbf{h}(\mathbf{x}_t) + \mathbf{e}_t \tag{2b}$$

and we will assume that the measurement errors are independent white Gaussian sequences.

The Bayesian way of looking at the estimation problem can be quite illustrative. It is well known that the optimal estimate in the linear and nonlinear cases is given by the conditional mean. The conditional probability density function (PDF) is given by

$$p(\mathbf{x} \mid \mathbf{y}) = \frac{p(\mathbf{y} \mid \mathbf{x}) p(\mathbf{x})}{p(\mathbf{y})} = \frac{L(\mathbf{y} \mid \mathbf{x}) p(\mathbf{x})}{\int_{R^2} L(\mathbf{y} \mid \mathbf{x}) p(\mathbf{x}) d\mathbf{x}} \tag{3}$$

where $\int_{R^2} L(\mathbf{y} \mid \mathbf{x}) p(\mathbf{x}) d\mathbf{x}$ can be interpreted as a normalizing constant. We call $L(\mathbf{y} \mid \mathbf{x}) = p(\mathbf{y} \mid \mathbf{x})$ the likelihood function and refer to $p(\mathbf{x} \mid \mathbf{y})$ as the posterior PDF, while $p(\mathbf{x})$ is referred to as the prior PDF.

The recursive procedure means that we will start from a given prior PDF that we will propagate according to the movement of the vehicle and the uncertainty of the movement. The movement can, for example, be determined from an INS system that has a specified uncertainty. We can denote the propagated, but not measurement updated, PDF as $p^-(\mathbf{x})$. The next step in the recursive procedure is to do the measurement update of $p^-(\mathbf{x})$ by multiplication of $p^-(\mathbf{x})$ and $L(\mathbf{y} \mid \mathbf{x})$ in order to arrive at the posterior PDF. In the following we will look at this in some more details.

A. Propagation of the PDF for the vehicle position

The first equation (1) describes how the position changes between two sampling events. Figure 3 illustrates this. The

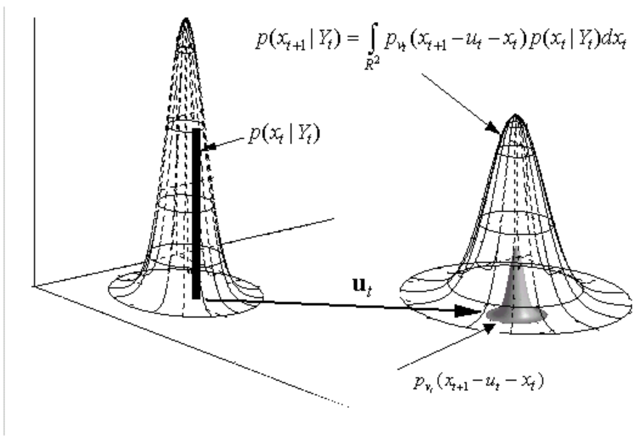

Fig. 3. Propagation of the PDF for the vehicle position.

left PDF (prior PDF) has a bearing upon the vehicle's position at sampling time t and the black pile is the relative frequency of the number of realizations which have ended in point $\mathbf{x}_t$, i.e. $p(\mathbf{x}_t \mid \mathbf{Y}_t)$. The notation $p(\cdot \mid \mathbf{Y}_t)$ indicates that the PDF is based on all measurements up to and including the measurement at time t. The realizations are moved the distance $\mathbf{u}_t$ but due to the uncertainty $\mathbf{v}_t$ we will have a spread in the new position. We multiply this new PDF - the small one in the figure - by the relative frequency $p(\mathbf{x}_t \mid \mathbf{Y}_t)$ and total the contributions of all points in the left PDF by an integral to get the position PDF at time t+1. We can express the propagation as

$$p(\mathbf{x}_{t+1} \mid \mathbf{Y}_t) = \int_{R^2} p_{\mathbf{v}_t}(\mathbf{x}_{t+1} - \mathbf{u}_t - \mathbf{x}_t) p(\mathbf{x}_t \mid \mathbf{Y}_t) d\mathbf{x}_t \tag{4}$$

where $p_{\mathbf{v}_t}(\cdot)$ is the PDF for the error term $\mathbf{v}_t$.

B. The measurement update

The measurement update is made according to (2b). We assume the error in the depth measurement to be Gaussian and independent. Therefore

$$L(\mathbf{y}_t|\mathbf{x}_t) = \frac{1}{\sqrt{(2\pi)^N \det(\mathbf{C}_e)}} e^{-\frac{1}{2}(\mathbf{y}_t - \mathbf{h}(\mathbf{x}_t))^T \mathbf{C}_e^{-1} (\mathbf{y}_t - \mathbf{h}(\mathbf{x}_t))} \tag{5}$$

where $\mathbf{C}_e$ is the measurement error covariance matrix. The function $L(\mathbf{y}_t \mid \mathbf{x}_t)$ is our likelihood function since, for a given position $\mathbf{x}_t$, it gives the likelihood of having the measurement value $\mathbf{y}_t$. The assumption that the error of different beams are uncorrelated makes the correlation matrix $\mathbf{C}_e$ diagonal and equal to $\sigma_e^2 \mathbf{I}$. Therefore the likelihood function will be

$$L(\mathbf{y}_t|\mathbf{x}_t) = \frac{1}{\sqrt{(2\pi\sigma_e^2)^N}} e^{-\frac{1}{2\sigma_e^2}\sum_{k=1}^{N}(y_{t,k} - h_k(\mathbf{x}_t))^2} \tag{6}$$

where $y_{t,k}$ and $h_k(\mathbf{x}_t)$ are the kth components of the vector $\mathbf{y}_t$ and $\mathbf{h}(\mathbf{x}_t)$, respectively.

Figure 4 shows the non-normalized likelihood function for a measurement with only one beam, which is the usual way that the measurement is done in terrain navigation. Figure 5 shows the likelihood function corresponding to a measurement with 9 x 9 beams. The size of the map is 4 x 4 km in both cases. It can be seen from the figures that using a large number of beams drastically reduces the number of likely positions.

The next step in the recursion is to fuse the likelihood function for the measurement with the propagated PDF of the position. The non-normalized posterior PDF is obtained as

$$p(\mathbf{x}_{t+1} \mid \mathbf{Y}_{t+1}) \sim L(\mathbf{y}_{t+1} \mid \mathbf{x}_{t+1}) p(\mathbf{x}_{t+1} \mid \mathbf{Y}_t) \tag{7}$$

The Figures 6 and 7 show the non-normalized measurement-updated PDF. A comparison between Figure 6 and 7 shows,

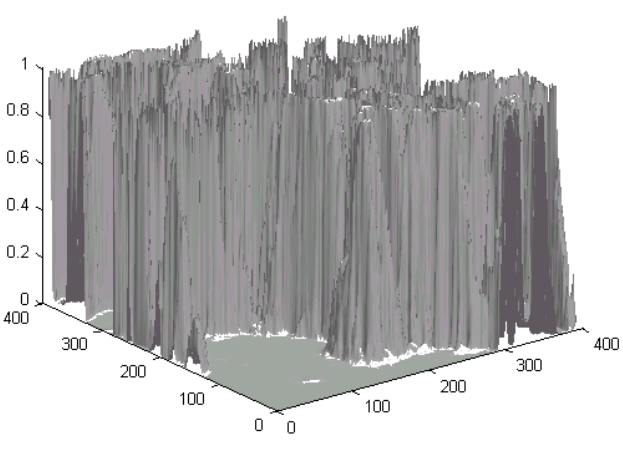

Fig.4. Likelihood function when using one measurement beam.

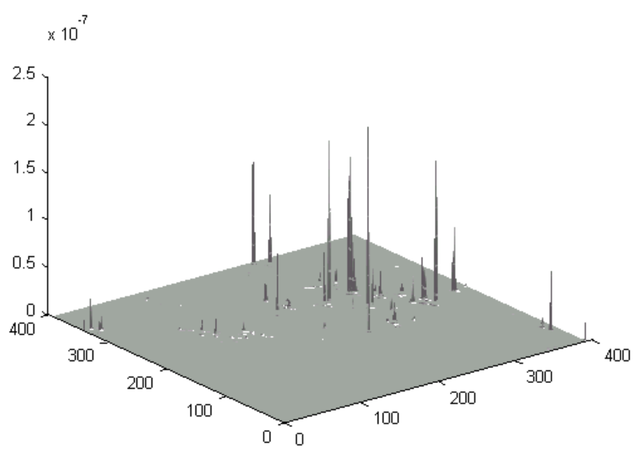

Fig.5. Likelihood function when using 9 x 9 measurement beams.

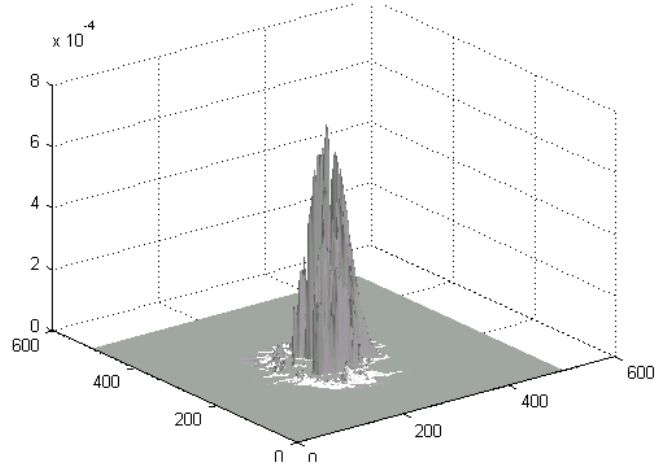

Fig.6. The measurement updated prior for one measurement beam.

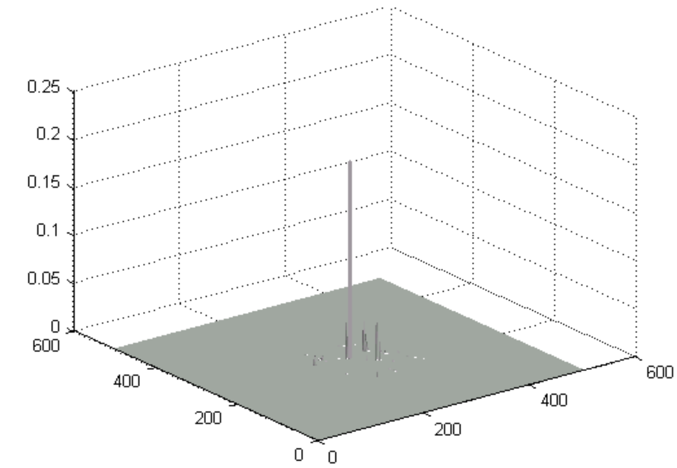

Fig. 7. The measurement updated prior for 9 x 9 measurement beams.

as expected, that the variance is much smaller when many beams are used in the measurement.

If the time between the measurements is large, the variance in the propagated PDF, $p^{-}(\mathbf{x})$, may increase such that it will not noticeably improve the estimation of the position based on the likelihood function. Hence, when the prior PDF has a large variance the estimation problem becomes a maximum likelihood (ML) estimation problem.

III. REDUCING FALSE POSITIONS

The Figure 4 shows several local maxima for the likelihood function but Figure 5 only a few. Those maxima are due to the fact that the bottom topography repeats itself. Since the vehicle only can be at one place at a time, we would like to reduce the number of false likelihood positions and we can see from Figures 4 and 5 that increasing the number of measurement beams is an effective method for achieving that.

Let us for simplicity study the problem with false positions in one dimension since it may be easily illustrated then [5]. Assume we have a stochastic bottom profile as in Figure 8. The sonar, which has N measurement beams, has measured the profile in area 1 and it is found to be

$$\mathbf{y} = \mathbf{h}_1 + \mathbf{e} \tag{8}$$

where $\mathbf{e}$ is the measurement error. Now we are comparing this measurement with the underwater map in area 2 which has the bottom profile $\mathbf{h}_2$. We will also, in the following, assume that the elements in the vectors $\mathbf{h}$ are a correlated Gaussian sequence. Let

$$\Delta\mathbf{h}=\mathbf{h}_1- \mathbf{h}_2. \tag{9}$$

Now we want to find the probability that the absolute value of the elements in the vector $|\Delta\mathbf{h}| < \varepsilon_h$ since that means that the two bottom profiles are very close to each other. The notation $|\Delta\mathbf{h}| < \varepsilon_h$ means that the absolute value of every element in the vector $\Delta\mathbf{h}$ should be smaller than ε_h. Since we assumed $\mathbf{h}$ to be Gaussian, we have

$$f(\Delta\mathbf{h}) = \frac{1}{(2\pi)^{N/2}\sqrt{|\mathbf{C}|}} e^{-\frac{1}{2}\Delta\mathbf{h}^T\mathbf{C}^{-1}\Delta\mathbf{h}} \tag{10}$$

where $\mathbf{C}$ is the covariance matrix of $\Delta\mathbf{h}$. The simplest way to calculate the probability that the two bottom profiles are close to each other may be to first decorrelate the vector $\Delta\mathbf{h}$ by a mode decomposition of the covariance matrix

$$\mathbf{C} = \mathbf{U\Lambda U}^T \tag{11}$$

where $\mathbf{U}$ is the eigenvector matrix and $\mathbf{\Lambda}$ is the eigenvalue matrix. Making the substitution $\Delta\mathbf{h} = \mathbf{Uy}$ means that an upper bound of the probability, that the difference in depth of the two places is less then a small number, is

$$P(|\Delta\mathbf{h}| \le \varepsilon_h) \le P(|\Delta\mathbf{y}| \le \varepsilon)$$
$$= \int_{-\varepsilon}^{\varepsilon}\cdots\int_{-\varepsilon}^{\varepsilon}\prod_{i=1}^{N}\frac{e^{-\frac{y_i^2}{2\lambda_i}}}{\sqrt{2\pi\lambda_i}}dy_1\cdots dy_N = \prod_{i=1}^{N}\int_{-\varepsilon}^{\varepsilon}\frac{e^{-\frac{y_i^2}{2\lambda_i}}}{\sqrt{2\pi\lambda_i}}dy_i \tag{12}$$

The hypercube ε encloses the hypercube ε_h. The covariance matrix is assumed to be positive definite, i.e. all eigenvalues $\lambda_i > 0$ so each factor

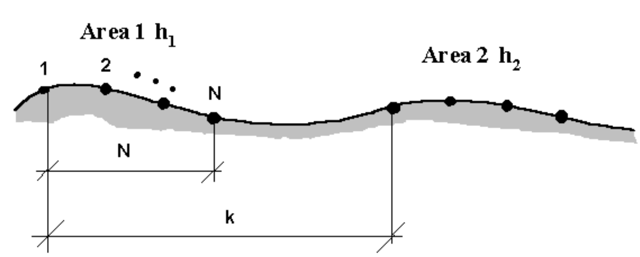

Fig. 8. A bottom profile section.

$$\int_{-\varepsilon}^{\varepsilon} \frac{e^{-\frac{y_i^2}{2\lambda_i}}}{\sqrt{2\pi\lambda_i}} dy_i < 1 \tag{13}$$

if $\varepsilon > 0$. The probability that the terrain repeats itself will thus decrease exponentially with N.

It is easy to show that the above conclusion is valid also for non-Gaussian correlated sequencies $\mathbf{h}$ since any PDF can be approximated as closely as desired by a sum av Gaussian PDFs $f_m(y)$, [6]. Equation (10) can therefore be written as

$$P(|\Delta\mathbf{h}| \le \varepsilon_h) \le P(|\mathbf{y}| \le \varepsilon)$$
$$= \int_{-\varepsilon}^{\varepsilon} \cdots \int_{-\varepsilon}^{\varepsilon} \sum_{m=1}^{M} f_m(y) d\mathbf{y} = \sum_{m=1}^{M} \int_{-\varepsilon}^{\varepsilon} \cdots \int_{-\varepsilon}^{\varepsilon} f_m(y) d\mathbf{y} \tag{14}$$

For every fix M the left side will exponentially approach zero when N increases above all bounds.

Figure 9 illustrates the exponential decrease in probability that the terrain repeats itself, according to (12), for two synthetic bottom profiles generated by passing white noise through an AR(1)-filter with a pole in a = 0.96 and a = 0.99.

An increase in the number of measurement beams not only decreases the number of false likelihood positions but it also makes the peak of the likelihood function much sharper.

We conclude from this section that with the number of measuring beams we typically are using the problem of a false position will not be a problem for bottom areas that are not extremely flat. This has also been the experience from our sea trials. When it occasionally still happens the simplest way to eliminate the problem is to increase the size of the total sonar footprint since the decrease in probability is exponential.

IV. MAXIMUM LIKELIHOOD ESTIMATION

We know from the theory of ML estimation that, under weak assumptions, the ML-estimate, [7] [8]

- is asymptotically unbiased
- asymptotically reaches the Cramér-Rao lower bound
- is asymptotically Gaussian distributed

The asymptotic covariance of the ML-estimate $\hat{\mathbf{x}}(\mathbf{y})$ can therefore be expressed as

$$\mathbf{R} = E\{[\hat{\mathbf{x}}(\mathbf{y}) - \mathbf{x}]^2\} = \mathbf{J}^{-1} \tag{15}$$

where $\mathbf{J}$ is Fisher's information matrix

$$\mathbf{J} = -E\{\frac{\partial^2[\ln p(\mathbf{y}\,|\,\mathbf{x})]}{\partial\mathbf{x}\partial\mathbf{x}^T}\} \tag{16}$$

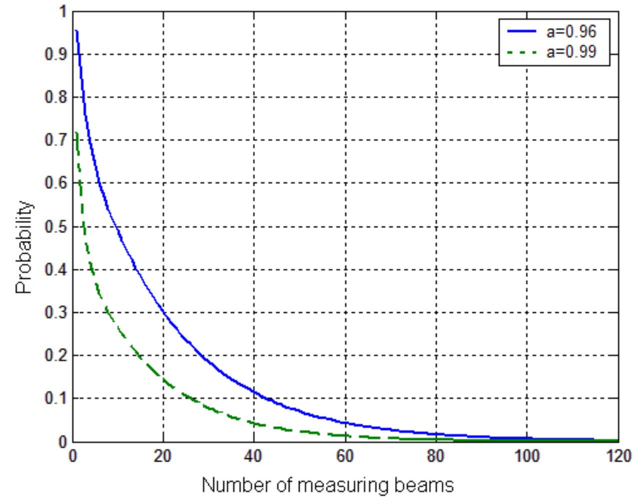

Fig. 9. Probability that the bottom repeats itself.

We have

$$\mathbf{R} = \sigma_e^2 \begin{bmatrix} \sum_{i=1}^{N} \left[\frac{\partial h_i}{\partial x_1}\right]^2 & \sum_{i=1}^{N} \frac{\partial h_i}{\partial x_1}\frac{\partial h_i}{\partial x_2} \\ \sum_{i=1}^{N} \frac{\partial h_i}{\partial x_2}\frac{\partial h_i}{\partial x_1} & \sum_{i=1}^{N} \left[\frac{\partial h_i}{\partial x_2}\right]^2 \end{bmatrix}^{-1} \tag{17}$$

where index i refers to the derivative at beam i and x_1, x_2 refer to the east and north directions, respectively.

The covariance in the position error estimate can thus be calculated in real time or in advance from the underwater map if so is wanted. We see from (17) that the error covariance is inversely proportional to the number of beams. Since the elements in the covariance matrix correspond to the slope of the bottom this also means that the method, with several measuring beams, can be used in much flatter bottom areas

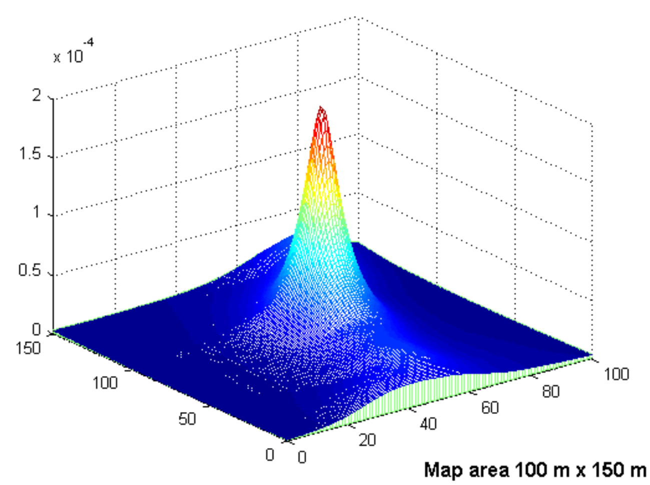

Fig. 10. Typical likelihood function. This is from the October 2002 sea-trial, WP3.

than the measuring with only one beam.

Of great interest in our case is the convergence of the normalized likelihood function towards the Gaussian PDF. Even if the exponent in our likelihood function (6) is quadratic in h(**x**) we expect it to be close to a Gaussian function with respect to **x**, see Figure 10.

Figure 11 shows the convergence of the Cramér-Rao lower bound, see (17), for way-point three in the October 2002 sea-trial described in SectionVI. Normally we use more than 150 measurement beams depending on the actual sonar. In the October 2002 sea-trial we used 400 beams so from Figure 11 we conclude we are close to the asymptotic value of the covariance matrix.

Figure 12 shows a comparison between the likelihood function and the Gaussian curve for real measurements and real maps with 400 measuring beams assembled from 5 beam planes. Data is from way-point three in the sea trial. Figure 13 shows a comparison between the likelihood functions based on the normalized correlation function (1) for different numbers of measuring beams. Note that the exponent in the likelihood function (6) has been normalized with respect to *N*.

In the legend box, for example, 400:5 means that the 3D sonar measurement is composed from 5 beam planes (pings). From the figure we see that even 15 beams still produce a good approximation of a Gaussian curve. The beams are assembled from 11, 5 and 3 beam planes, respectively. Assembling beams from beam planes instead of using a true 3D sonar introduces errors resulting from errors in the relative distance and orientation of the beam planes. That is the reason why 800 and 400 beams produce a greater variance than the others in Figure 13. We usually assembled 400 beams from 5 beam planes in the October sea-trial.

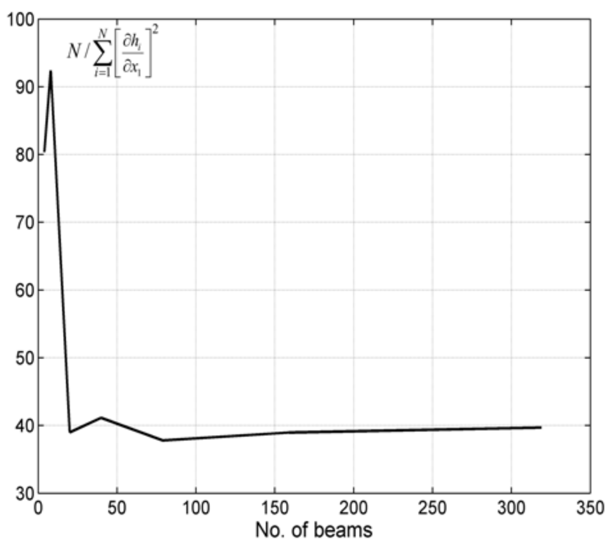

Fig. 11. The convergence of the Cramér-Rao bound as a function of the number of measurement beams. Data from WP3 in the October 2002 sea-trial.

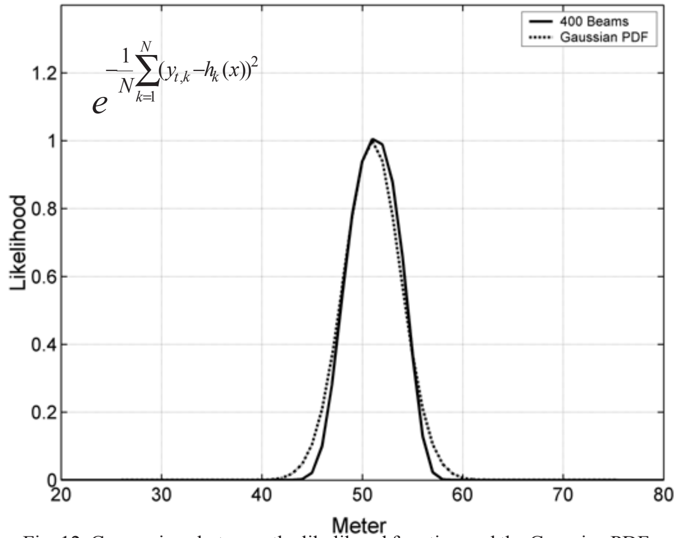

Fig. 12. Comparison between the likelihood function and the Gaussian PDF. Data from WP3 the October 2002 sea-trial. Cf. Figure 10.

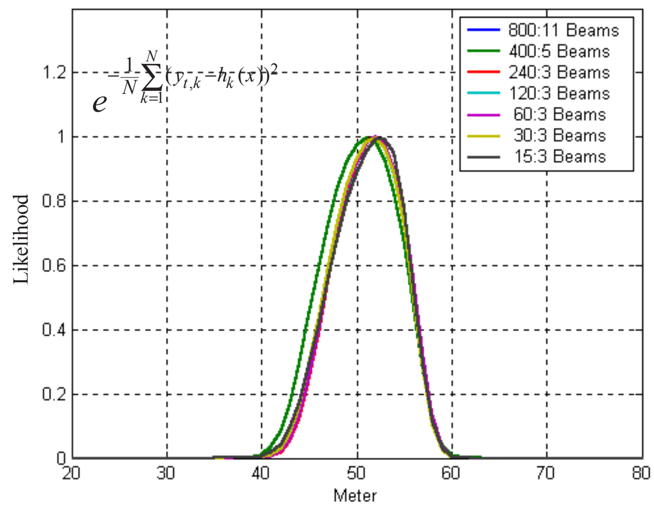

Fig. 13. Comparison between the likelihood functions for different numbers of measurement beams.

It is known that if a large number of continuos functions, of a certain class, are succesively self-multiplied the result may approach the Gaussian form [9], [10]. This can be explained by the central limit theorem and the functions need not be all the same. This will apply to our likelihood function (6). The complete requirements for the convergence towards a Gaussian PDF when *N* increases above all bounds can be found in [10]. The covariance (17) of the Gaussian PDF will be proportional to the radius of curvature at the peak in Figure 10.

We conclude from above that assuming the likelihood function to be Gaussian and with a covariance according to (17) will only amount to a small approximation. Thus we will be able to formulate a linear optimal Kalman filter for fusing the prior propagated position PDF with the likelihood function.

V. THE LINEAR KALMAN FILTER

In order to formulate the linear Kalman filter we redefine our measurement equation (2b)

$$\mathbf{x}_{t+1} = \mathbf{x}_t + \mathbf{u}_t + \mathbf{v}_t \qquad t = 1,2,3...$$

$$\mathbf{z}_t = \mathbf{x}_t + \mathbf{w}_t \tag{18}$$

Here $\mathbf{z}_t$ is our measured position given by the correlation between the sonar map and the underwater map, the ML-estimate, and the error term $\mathbf{w}_t$ is assumed to be a white sequence with zero mean. The covariance of $\mathbf{w}_t$ is given by (17).

In the following, as before, the superscript $-$ means the quantity before measurement update. The INS-system is assumed to be reset after each determination of the position. The prior estimated position, $\mathbf{x}_t^-$, the propagation step in the Kalman recursive algorithm, will therefore directly be given by the INS-system [11].

For the linear Kalman filter we assume the following covariance matrix for the prior PDF

$$\mathbf{Q}_t = E\{\mathbf{v}_t \mathbf{v}_t^{\,T}\} \tag{19}$$

Due to irregular sampling it will be time dependent [11]. Our measurement updated position will be

$$\hat{\mathbf{x}}_t = \mathbf{x}_t^- + \mathbf{K}_t(\mathbf{z}_t - \mathbf{x}_t^-) \tag{20}$$

where the Kalman gain is

$$\mathbf{K}_t = \mathbf{P}_t^- \left(\mathbf{P}_t^- + \mathbf{R}_t\right)^{-1} \tag{21}$$

and the covariance of the propagated old posterior position estimate

$$\mathbf{P}_t^- = \mathbf{P}_{t-1} + \mathbf{Q}_t \tag{22}$$

The covariance for the measurement updated position is given by

$$\mathbf{P}_t^{-1} = (\mathbf{P}_t^-)^{-1} + \mathbf{R}_t^{-1} \tag{23}$$

Note that, when we have a low informative prior position PDF we have $\mathbf{P}_t \approx \mathbf{R}_t, \mathbf{K}_t = \mathbf{I}, \hat{\mathbf{x}}_t = \mathbf{z}_t$.

Since the normalized likelihood function is very close to the Gaussian PDF, the filter will be almost optimal. It can also be worth noting that a larger number of measurement beams makes the propagation stage more robust to modelling errors in the propagation. This can be seen from Figure 6. An error in the propagation of the prior PDF will select a wrong part of the likelihood function for calculating the position estimate and the posterior PDF's covariance. As can be seen from Figure 7 an error in the propagation will have a very low influence on the position estimate of the position when we have a larger number of measurement beams.

An important side effect of the linearization is that the presented method easily can be applied to a more general process model [12]

$$\mathbf{x}_{t+1} = \mathbf{F}_t \mathbf{x}_t + \mathbf{G}_t \mathbf{u}_t + \mathbf{\Gamma}_t \mathbf{v}_t \tag{24}$$

with the state vector extended to include the state variables of the INS-system and thus avoiding the complication with Rao-Blackwellization as in the particle filter [12][13].

VI. SEA TRIALS

A number of sea-trials have been conducted to verify the theoretical results. The magnitude of the position error of course depends on the flatness of the sea bottom. In the north part of the Baltic Sea we have achieved in simulations 1σ - circular position errors, due to only the measurement noise, in the 0.3 – 0.4 meter range. It should, however, be noted that there are several other sources of position errors that can be of greater concern than position error due to measurement noise.

Such error may result from misalignment and incomplete calibration of the sonar equipment, or incomplete corrections for the vehicles motion in terms of roll, pitch and heave. Other types of error are vertical and horizontal map errors and DGPS errors if DGPS is used as a position reference.

A sea-trial were conducted in October 2002 in the Stockholm archipelago in Sweden. A 65 km long track with 8 way-points, where the ship position at each way-point was determined by correlation, was laid out. The Reson 8101 bathymetric sonar was used and 5 beam-planes, about 12 meters apart, with 80 valid beams each, were assembled to form a 3D-bathymetric measurement of the bottom. Depending on the depth at the actual way-point the area that where ensonified was about 100 x 100 meter to 200 x 200 meter.

Figure 14 shows the underwater landscape at way-point 3. The map-area is 5 x 5 km and the blue pile shows the pre-selected way-point.

Intensive Monte Carlo simulations of the position accuracy were done before the sea-trial. Figure 15 shows the likelihood function from a Monte Carlo run. Figure 16 shows the position error from the Monte Carlo simulation. In 3 % of

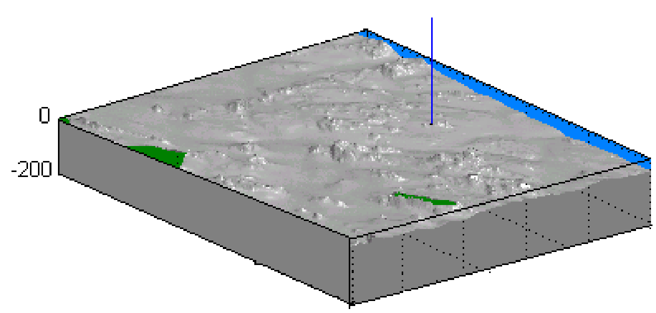

Fig. 14. Underwater map, 5 km x 5 km, at way-point three. The blue vertical pole indicates WP3. The vertical scale is enlarged 25 times.

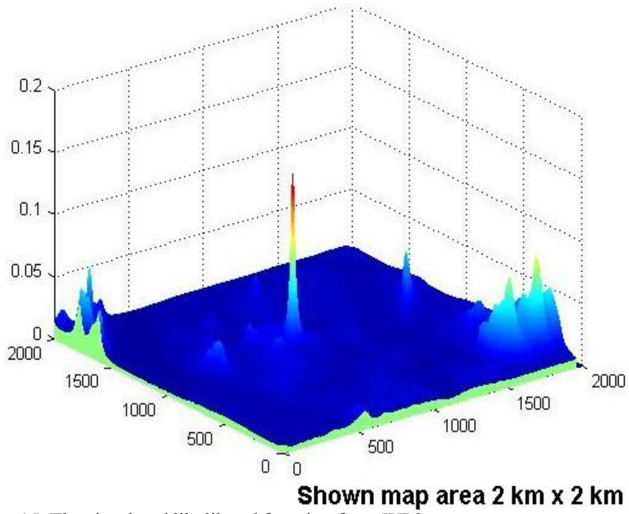

Fig. 15. The simulated likelihood function from WP3.

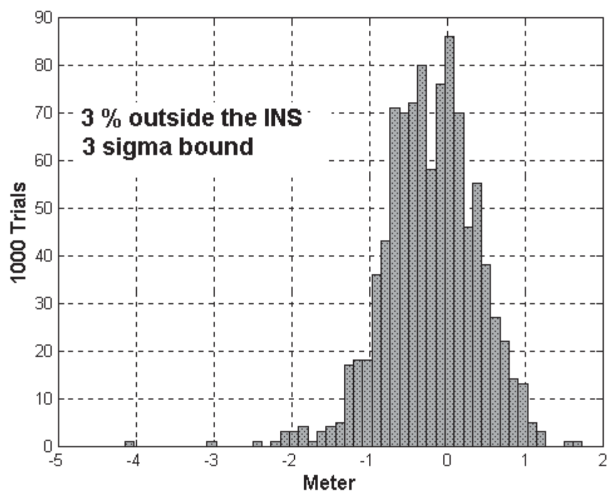

Fig. 16. Position error at WP3 in the easterly direction.

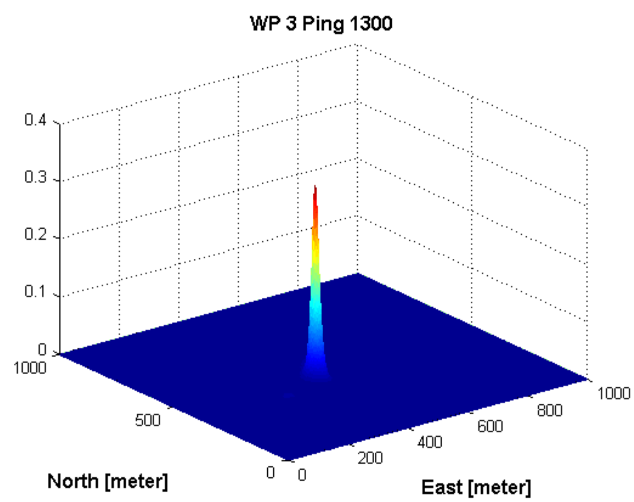

Fig. 17. The measured likelihood function at WP3.

all runs we were not able to establish a position within the 3σ - circular position error of the INS-system. Figure 17 shows the measured likelihood function at way-point three. It should be compared with Figure 15.

VII. CONCLUSIONS

It has been shown that using a sonar with many measurement beams in terrain navigation both accuracy and robustness will considerably increase. The position can also in many cases be determined without a prior PDF for the position.

Another main advantage with the correlation method is that a linear Kalman filter can be used without the problems that are associated with the extended Kalman filter, the mass-point filter or the particle filter. This implies in particular that extra states for the estimation of the INS bias parameters can easily be added.

ACKNOWLEDGMENT

The authors would like to thank Mr. Carl-Johan Andersson and CDR. Stefan Ahlberg at The Material Administration, FMV, Sweden for their support of this research project.

Thanks are also due to the Reson Company and Technical Director T. Meurling, MSc., and Sales Manager Navy C. W. Glädesdahl, MSc., and Hydrographer R. Hill, BSc., for their kind support during the sea trial. Reson personnel collected the bathymetric data during the sea trial.

REFERENCES

[1] L. D. Hostetler, R. D. Andreas,“Nonlinear Kalman Filtering Techniques for Terrain-Aided Navigation” in H.W. Sorensen, editor, *Kalman filtering: Theory and Application,* IEEE Press 1985.

[2] A. J. Robins, “Recent Developments in the TERPROM Integrated Navigation System”, Proceedings of the 44th Annual ION Meeting. Annapolis, Maryland. June 1988.

[3] O. Bergem,“ Bathymetric Navigation of Autonomous Underwater Vehicles using a Multibeam Sonar and a Kalman Filter with Relative Measurement Covariance Matrices”, Dr. Scient thesis, University of Trondheim, Norway, 1993.

[4] N. Bergman, “Recursive Bayesian Estimation, Navigation and Tracking Applications”, PhD thesis, Department of Electrical Engineering, Linköping University, Linköping, Sweden. 1999.

[5] I.Nygren, ”A Method for Terrain Navigation of an AUV”, Conference proceedings, MTS/IEEE Oceans 2001.

[6] B. D. O. Anderson, J. B. Moore, *Optimal Filtering,* Prentice Hall 1979.

[7] Steven M. Kay, *Fundamentals of Statistical Signal Processing, Estimation Theory*, Prentice Hall 1993.

[8] H.L. Van Trees, *Detection, Estimation and Modulation Theory*. Wiley, New York,1968.

[9] R. N. Bracewell, *The Fourier Transform and Its Applications*. Second edition, revised, MacGraw-Hill, 1986.

[10] A. I. Khinchin, *Matematical Foundations of Statistical Mechanics*, Dover Publications, Inc., New York, 1949.

[11] R. G. Brown, P. Y. C. Hwang, *Introduction to Random Signals and Applied Kalman Filtering*, John Wiley & Sons 1997.

[12] F. Gustavsson, F. Gunnarsson, N. Bergman, U. Forssell, J. Jansson, R. Karlsson, P.-J. Nordlund, “Particle Filters for Positioning, Navigation, and Tracking”. IEEE Transactions on Signal Processing, Vol. 50, No 2,pp. 425-437, 2002.

[13] K. Murphy, S. Russel,“Rao-Blackwellised Particle Filtering for Dynamic Bayesian Networks” in A. Doucet, N. de Freitas, N. Gordon, editors, *Sequential Monte Carlo Methods in Practice*, Springer 2001.